J Neural Transm (2013) 120:853–858
DOI 10.1007/s00702-012-0954-0

In silico identification of novel and selective monoamine oxidase B inhibitors

Kemal Yelekçi · Bora Büyüktürk · Nurdan Kayrak

Received: 11 October 2012 / Accepted: 4 December 2012 / Published online: 15 December 2012

Abstract Monoamine oxidases (MAO) A and B are flavin adenine dinucleotides containing enzymes bound to the mitochondrial outer membranes of the cells of the brain, liver, intestine, and placenta, as well as platelets. Recently, selective MAO-B inhibitors have received increasing attention due to their neuroprotective properties and the multiple roles they can play in the therapy of neurodegenerative disorders. This study was based on 10 scaffolds that were selected from more than a million lead compounds in the ZINCv12 lead library for their structural and physicochemical properties which inhibit MAO-B. Utilizing ZINC and Accelrys 3.1 fragment-based libraries, which contain about 400 thousand fragments, we generated 200 potential candidates. GOLD, LibDock, and AutoDock 4.02 were used to identify the inhibition constants and their position in the active sites of both MAO isozymes. The dispositions of the candidate molecules within the organism were checked with ADMET PSA 2D (polar surface area) against ADMET AlogP98 (the logarithm of the partition coefficient between *n*-octanol and water). The MAO-B inhibition activities of the candidates were compared with the properties of rasagiline which is known to be a selective inhibitor of MAO-B.

Keywords Monoamine oxidase (MAO-A, MAO-B) · Inhibition · In silico screening · Molecular modelling · Docking · De novo design · Selective inhibitors

K. Yelekçi (✉) · B. Büyüktürk · N. Kayrak
Department of Bioinformatics and Genetics,
Faculty of Engineering and Natural Sciences,
Kadir Has University, 34083 Fatih, Istanbul, Turkey
e-mail: kyelekci@gmail.com

Introduction

Monoamine oxidases (MAO) A and B are flavin adenine dinucleotides (FAD) containing enzymes bound to the mitochondrial outer membrane of the cells of the brain, liver, intestine, and placenta, as well as and platelets (Weyler et al. 1990). The basic difference between these two isozymes is their selectivity for the oxidation of various substrates and inhibitors. MAO-A preferentially deaminates serotonin (5HT) and norepinephrine (NE), and is selectively inhibited by clorgyline. On the other hand, MAO-B preferentially deaminates β-phenylethylamine (PEA) and benzylamine, and is selectively and irreversibly inhibited by *R*-deprenyl. Dopamine, tryptamine, and tyramine are common substrates for MAO-A and MAO-B (Holtzheimer and Nemeroff 2006).

The oxidation mechanism of MAOs has not yet been clearly established. However, several mechanisms have been proposed for amine oxidation (Silverman et al. 1982). These mechanisms include single electron transfer (Yelekci et al. 1989), direct hydride transfer from the amine substrate to flavin, and polar nucleophilic addition to flavin (Wang and Edmondson 2011; Edmondson et al. 2007; Erdem et al. 2006; Borstnar et al. 2011). MAOs play an important role in the catabolism of monoamine neurotransmitters, and as a result MAO inhibitors (MAOI) are critical for the treatment of several psychiatric and neurological diseases. MAO-B inhibitors are used in the treatment of Parkinson's and Alzheimer's diseases, whereas MAO-A inhibitors are used in antidepressant and anti-anxiety drugs (Binda et al. 2007; Youdim et al. 2006). Both MAO-A and MAO-B are crucial for the development of more selective and reversible MAO inhibitors. For many years, pyrazoline derivatives have been widely used (Gökhan-Kelekçi et al. 2009). Recently, selective MAO-B

inhibitors have received greater attention for the multiple roles they can play in the therapy of neurodegenerative disorders and for their neuroprotective properties (Weinreb et al. 2010). Although the numerous MAO-A inhibitors having important therapeutic potential against depression have been synthesized since last 50 years, few examples of selective MAO-B inhibitors are available. Nonetheless, there is still a need for the design of more potent, more selective and reversible monoamine oxidase inhibitors. The published crystallographic structures of MAO-A (Son et al. 2008) and MAO-B (Binda et al. 2007) isozymes have paved the way for computational modeling and drug design studies.

Numerous computational modeling and docking studies have been carried out with the aim of obtaining additional validation and support for the experimental results obtained for MAO-A and MAO-B by us and other researchers (Toprakci and Yelekci 2005; Erdem et al. 2006; Chimenti et al. 2007; Harkcom and Bevan 2007; Yelekci et al. 2007).

This study was based on 10 scaffolds (Fig. 1) that were selected from more than a million lead compounds in the ZINCv12 lead library for their structural and physico-chemical properties which inhibit MAO-B (Irwin and Shoichet 2005). Among those leads rasagiline type scaffolds were chosen for optimization since rasagiline is being used clinically as an antiparkinson and neuroprotective drug. Utilizing ZINC and Accelrys 3.1 fragment-based libraries, which contain about 400 thousand fragments, we generated 200 potential candidates (Scheme 1). GOLD, LibDock, and AutoDock 4.02 were used to identify the inhibition constants and their position in the active sites of both MAO isozymes. The dispositions of the candidate molecules within the organism were checked with ADMET PSA 2D (polar surface area) against ADMET AlogP98 (the logarithm of the partition coefficient between *n*-octanol and water (Fig. 6.). The MAO-B inhibition activities of the candidates were compared with the properties of rasagiline which is known to be a selective inhibitor of MAO-B.

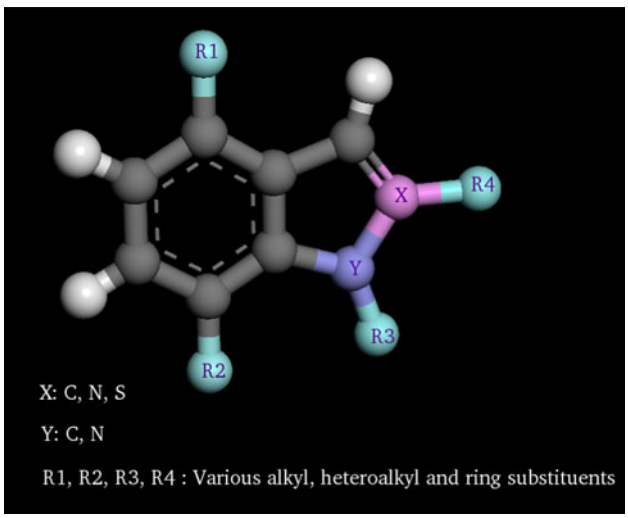

Fig. 1 Lead scaffold used in this study

Materials and methods

For this study, the crystal structures of MAO-A and MAO-B were obtained from the Protein Data Bank (PDB) [http://www.rcsb.org. For the MAO-A pdb code: 2Z5X; human monoamine oxidase in complex with harmine, resolution 2.2 Å (Son et al. 2008) and for the MAO-B pdb code: 2V5Z; human MAO-B in complex with the inhibitor safinamide, resolution 1.6 Å (Binda et al. 2007)]. Each

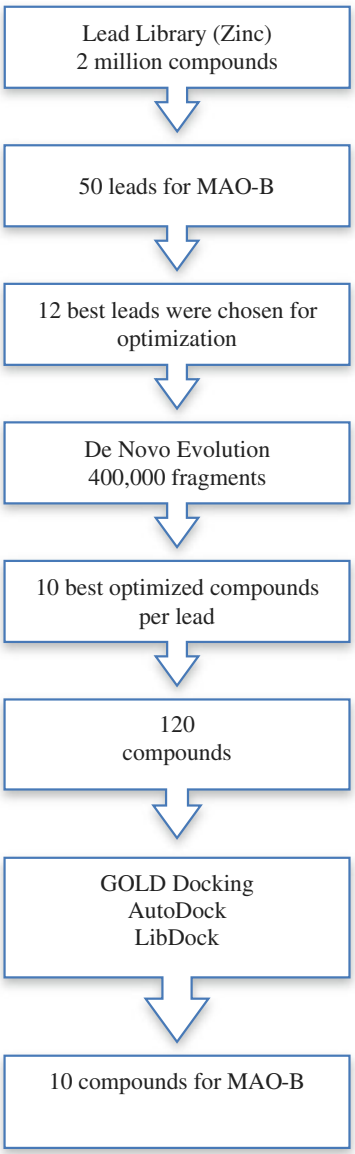

Scheme 1 Screening process

structure was cleaned of all water molecules and inhibitors as well as all non-interacting ions before being used in the docking studies. When the inhibitor was covalently bound to the FAD, the initial oxidized form of the FAD was used. For MAO-A and MAO-B, one of the two subunits was taken as the target structure. Using a fast Dreiding-like force field, each protein's geometry was first optimized and then submitted to the "Clean Geometry" toolkit of Discovery Studio (Accelerys Inc.) for a more thorough check. Missing hydrogen atoms were added based on the protonation state of the titratable residues at a pH of 7.4. Ionic strength was set to 0.145 and the dielectric constant was set to 10.

Generation of potential inhibitors

The design approach was based on the structure of the active site cavities of MAO-A and MAO-B. The scaffolds were used for the derivation of leads using the commercial software de Novo *Design* from the module of the Accelrys' program. The GOLD, LibDock, and AutoDock 4.2, AutoDock Tools (ADT) (Morris et al. 1998; Huey et al. 2007; Morris et al. 2009) programs were used for molecular docking into the active site of MAO-A and MAO-B isozymes. The rasagiline used in this study, which has a structural similarity to our scaffolds, was also derived from the literature to facilitate a comparison of its reported experimental inhibition constant values with those that we obtained computationally. Table 1 lists all 10 potential inhibitors as well as rasagiline (the experimental inhibition constants of rasagiline are 9.7 μM and 0.7 μM for MAO-A and MAO-B, respectively) (Hubálek et al. 2004) and their computational physicochemical properties for MAO-A and MAO-B. Scheme 2 shows their chemical structures.

Rasagiline	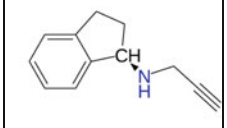	**6**	
1	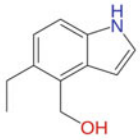	**7**	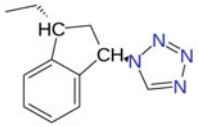
2	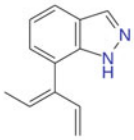	**8**	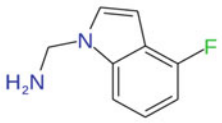
3	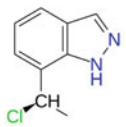	**9**	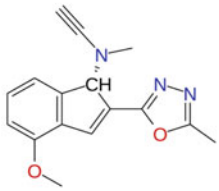
4	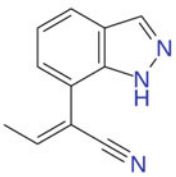	**10**	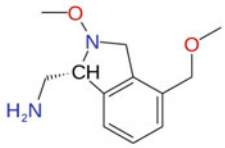
5	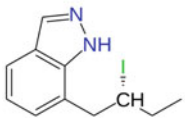		

Scheme 2 Chemical structures of 10 best-designed MAO-B inhibitors

Table 1 Inhibition constants and scores of 10 best-designed MAO-B inhibitors

Inhibitors	AutoDock inhibition constants		LibDock scores		GOLD scores	
	MAO-A (μM)	MAO-B (μM)	MAO-A	MAO-B	MAO-A	MAO-B
Rasagiline	17.46	5.09	84.91	97.78	47.17	48.30
1	16.19	7.83	88.20	102.99	51.03	55.17
2	27.77	3.41	84.99	94.86	42.78	53.70
3	37.02	9.09	77.19	92.17	44.99	48.67
4	10.90	3.78	80.15	90.55	47.42	50.31
5	8.57	5.47	87.15	108.65	47.82	60.25
6	12.08	1.06	82.38	131.60	52.61	52.40
7	2.89	1.01	90.95	115.34	50.12	52.33
8	3.72	1.76	94.03	135.62	46.90	51.51
9	20.49	7.44	90.82	110.14	51.80	52.70
10	65.21	38.29	78.85	91.03	43.92	50.86

Results and discussion

To render visible the detailed interactions of the docked poses of the designed inhibitors, the compound **1** was selected. Analysis of the optimal binding mode for the compound **1** (Figs. 2, 3) in the MAO-A active site cavity revealed that this compound is located in the vicinity of the FAD cofactor. The compound **1** interacts with active site residues lining the cavity as well as the FAD cofactor. The first hydrogen bond occurs between the amide group of the ILE207 and the hydroxy moiety of the **1**. The second hydrogen bond forms between the hydroxy group of the TYR444 and the hydroxy group of the **1**, and the last hydrogen bond interaction occurs between the amine hydrogen of the **1** and the FAD cofactor. In addition to these significant interactions, two p–p interactions were found between the side chain of TYR407 and the two rings of the inhibitor **1**. The binding mode adopted by compound **1** fits snugly within a cavity lined with hydrophobic amino acid residues. This hydrophobic pocket includes PHE208, ILE335, LEU337, ILE180, PHE352, and TYR69 amino acids. GLN215 and ASN181 contribute to the other polar attractions.

Figures 4 and 5 show the poses of **1** in the active side of MAO-B in 3D and 2D depictions, respectively. The Indol ring of **1** is sandwiched tightly between the TYR398 and TYR435 phenyl rings comprising the hydrophobic cage in the active site of the MAO-B enzyme. This tightness

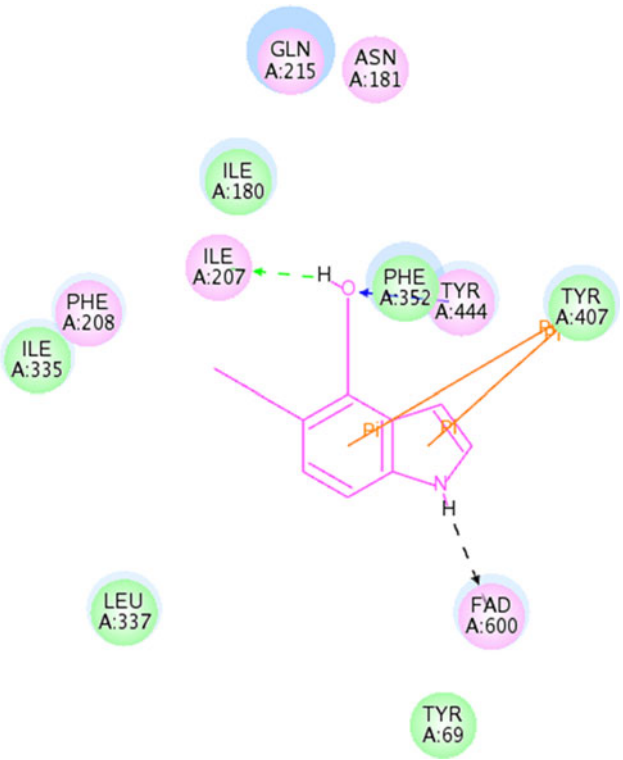

Fig. 3 The 2-dimensional depiction of compound **1** in the active site of the MAO-A enzyme. Residues involved in hydrogen bonding or polar interactions are represented by *magenta-colored circles*, and residues involved in vdW and hydrophobic interactions are shown by *green circles* in all 2-dimensional figures

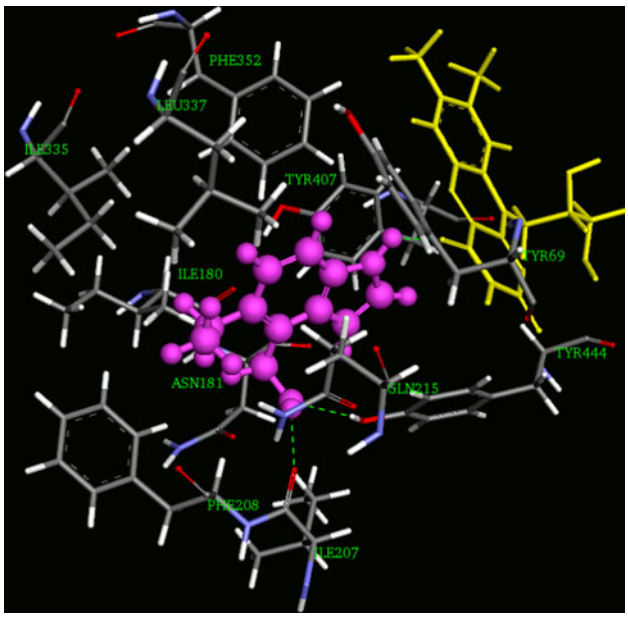

Fig. 2 The 3-dimensional orientation of compound **1** in the active site of the MAO-A enzyme. Amino acid side chains are shown as *sticks*, the inhibitor is shown as a *ball* and *stick* (*magenta*), and the cofactor FAD is depicted as a *yellow stick*

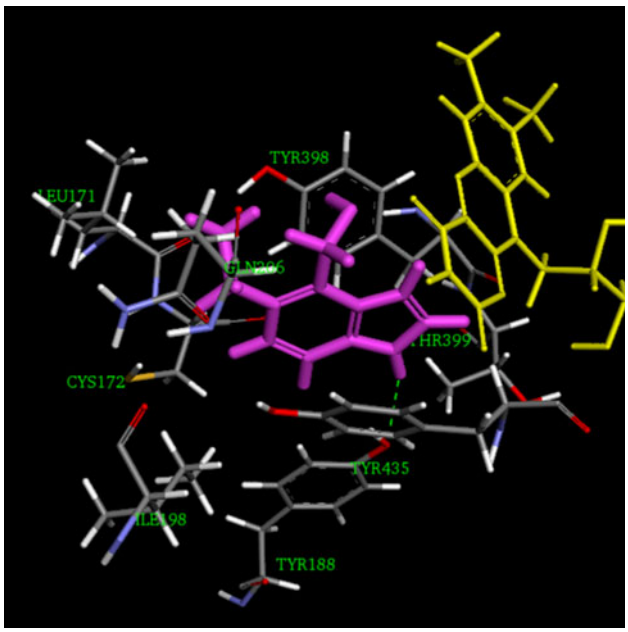

Fig. 4 The 3-dimensional orientation of compound **1** in the active site of the MAO-B enzyme. Amino acid side chains are shown as *sticks*, the inhibitor is shown as a *ball* and *stick*, and the cofactor FAD is depicted as a *yellow stick*

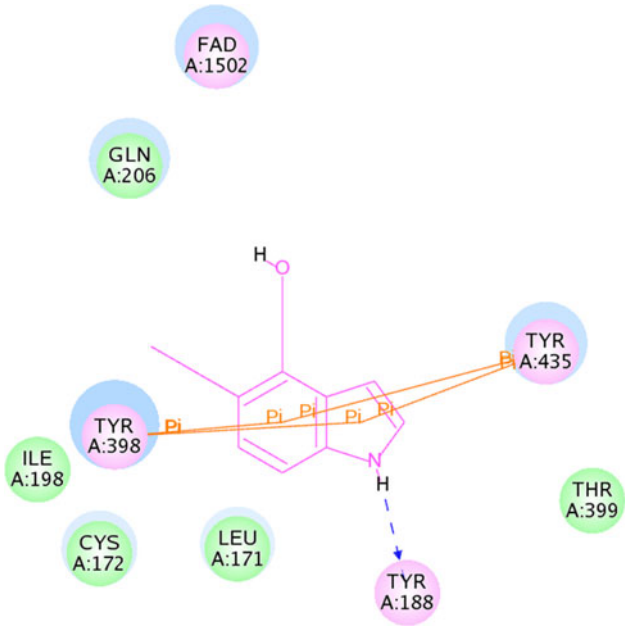

Fig. 5 2-dimensional depiction of compound **1** in the active site of the MAO-B enzyme. Residues involved in hydrogen bonding or polar interactions are represented by *magenta-colored circles*, and residues involved in vdW and hydrophobic interactions are shown by *green circles* in all 2-dimensional figures

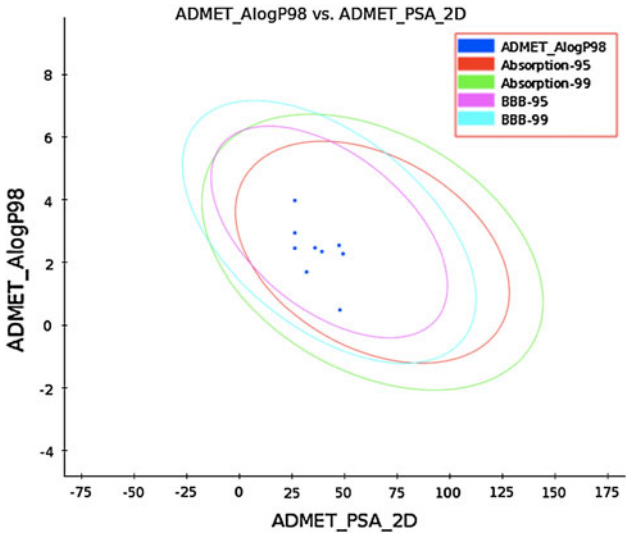

Fig. 6 ADMET plot. ADMET PSA 2D (polar surface area) versus ADMET AlogP98 (the logarithm of the partition coefficient between *n*-octanol and water)

originates from the four π–π interactions resulting from the indol ring and two tyrosine side chains. Another major interaction is the hydrogen bond that forms between the N–H hydrogen of the indol ring and hydroxy moiety of TYR188. In MAO-B, a hydrophobic pocket lined by ILE198, CYS172, LEU171, THR399, GLN206, and FAD surround the inhibitor **1**.

The selectivity and potency of the **1** molecule on MAO-B compared to MAO-A can be evaluated from the above data, indicating that the indol core is stabilized by four π–π interactions in MAO-B compared to only two π–π bonds in MAO-A. GOLD and LibDock docking tools also support these observations, as seen in Table 1. All of this data may suggest why the MAO-B inhibitory potency of compound **1** (Ki = 7.83 μM) is much better and more selective in comparison to MAO-A (Ki = 16.19 μM).

Conclusion

The computational results carried out with all of the docking tools clearly demonstrate that rasagiline (N-propargyl 1(R)-aminoindan) selectively inhibits MAO-B with respect to the MAO-A enzyme, which is in agreement with the reported experimental results. Our current design and computational evaluation of 10 potential MAO-B selective inhibitors using various docking tools are listed in Table 1 and Scheme 2. Newly designed inhibitors resulted in an almost fivefold improvement of inhibitory activity with respect to rasagiline. Small differences in the conformations and amino acid sequences of the two isozymes around their FAD regions, as discussed above, were the determining factors for the selectivity and the potency of the compounds. In addition, the newly designed inhibitors showed excellent ADMET properties. The computer-aided drug design of novel drug candidates for MAO-B, as reported in this study, represents a starting point for the synthesis of novel and selective MAO-B inhibitors.

Acknowledgments This research was supported by The Scientific and Technological Research Council of Turkey (TUBITAK), grant number 108T232.

References

Binda C, Wang J, Pisani L, Caccia C, Carotti A, Salvati P, Edmondson DE, Mattevi A (2007) Structures of human monoamine oxidase B complexes with selective noncovalent inhibitors: safinamide and coumarin analogs. J Med Chem 50:5848

Borstnar R, Repic M, Krzan M, Mavri J, Vianello R (2011) Irreversible inhibition of monoamine oxidase B by the antiparkinsonia medicines rasagiline and selegiline: a computational study. Eur J Org Chem 2011(32):6419–6433

Chimenti F, Maccioni E, Secci D, Bolasco A, Chimenti P, Granese A, Befani O, Turini P, Alcaro S, Ortuso F, Cardia MC, Distinto S (2007) Selective inhibitory activity against MAO and molecular modeling studies of 2-thiazolylhydrazone derivatives. J Med Chem 50:707–712

Edmondson DE, Binda C, Mattevi A (2007) Structural insights into the mechanism of amine oxidation by monoamine oxidases A and B. Arch Biochem Biophys 464:269–276

Erdem SS, Karahan Ö, Yildiz I, Yelekci K (2006) A computational study on theamine-oxidation mechanism of monoamine oxidase:

insight into the polar nucleophilic mechanism. Org Biomol Chem 4(4):646–658

Gökhan-Kelekçi N, Koyunoglu S, Yabanoglu S, Yelekçi K, Özgen Ö, Uçar G, Erol K, Kendi E, Yesilada A (2009) New pyrazoline bearing 4(3**H**)-quinazolinone inhibitors of monoamine oxidase Synthesis, biological evaluation, and structural determinants of MAO-A and MAO-B selectivity. Bioorg Med Chem 17:675–689

Harkcom WT, Bevan DR (2007) Molecular docking of inhibitors into monoamine oxidase B. Biochem Biophys Res Commun 360:401–406

Holtzheimer PE, Nemeroff CB (2006) Advances in the treatment of depression. NeuroTherapeutics 3:42–56

Hubálek F, Binda C, Li M, Herzig Y, Sterling J, Youdim MB, Mattevi A, Edmondson DE (2004) Inactivation of purified human recombinant monoamine oxidases A and B by rasagiline and its analogues. J Med Chem 47(7):1760–1766

Huey R, Morris GM, Olson AJ, Goodsell DS (2007) A semi-empirical free energy force field with charge-based desolvation. J Comp Chem 28(6):1145–1152

Irwin JJ, Shoichet BK (2005) ZINC—a free database of commercially available compounds for virtual screening. J Chem Inf Model 45(1):177–182

Morris GM, Goodsell DS, Halliday RS, Huey R, Hart WE, Belew RK, Olson AJ (1998) Automated docking using a Lamarckian genetic algorithm and an empirical binding free energy function. J Comp Chem 19(14):1639–1662

Morris GM, Huey R, Lindstrom W, Sanner MF, Belew RK, Goodsell DS, Olson AJ (2009) Autodock4 and AutoDockTools4: automated docking with selective receptor flexibility. J Comput Chem 16:2785–2791

Silverman RB, Hoffman SJ, Catus WBA III (1982) Mechanism for mitochondrial monoamine oxidase catalyzed amine oxidation. J Am Chem Soc 102:7126–7128

Son S-Y, Ma J, Kondou Y, Yoshimura M, Yamashita E, Tsukihara T (2008) Structure of human monoamine oxidase A at 2.2 Å resolution: the control of opening the entry for substrates/inhibitors. PNAS 105(15):5739–5744

Toprakci M, Yelekci K (2005) Docking studies on monoamine oxidase-B inhibitors: estimation of inhibition constants (**K**i) of a series of experimentally tested compounds. Bioorg Med Chem Lett 15:4438–4446

Wang J, Edmondson DE (2011) ^{2}H kinetic isotope effects and pH dependence of catalysis as mechanistic probes of rat monoamine oxidase A: comparisons with the human enzyme. Biochemistry 50:7710–7717

Weinreb O, Amit T, Bar-Am O, Youdim MBH (2010) Rasagiline: a novel anti-Parkinsonian monoamine oxidase-B inhibitor with neuroprotective activity. Prog Neurobiol 92:330–344

Weyler W, Hsu YP, Breakefield XO (1990) Biochemistry and genetics of monoamine oxidase. Pharmacol Ther 47:391–417

Yelekci K, Lu X, Silverman RB (1989) Electron-spin resonance studies of monoamin oxidase-B 1st direct evidence for a substrate radical intermediate. J Am Chem Soc 111:1138–1140

Yelekci K, Karahan Ö, Toprakci M (2007) Docking of novel reversible monoamine oxidase-B inhibitors: efficient prediction of ligand binding sites and estimation of inhibitors thermodynamic properties. J Neural Transm 114:725–732

Youdim MBH, Edmondson D, Tipton KF (2006) The therapeutic potential of monoamine oxidase inhibitors. Nat Rev Neurosci 7:295–309